

Discrete-Level Broadband Excitation Signals: Binary/Ternary Chirps

T. Paavle, M. Min

Th. J. Seebeck Dept. of Electronics, Tallinn University of Technology,
Ehitajate tee 5, 19086 Tallinn, Estonia, phone: +372 6201156, e-mail toivo@elin.ttu.ee

crossref <http://dx.doi.org/10.5755/j01.eee.122.6.1815>

Introduction

Chirps (fast frequency sweeps) and chirp-like signals have become popular excitation signals in measurement techniques, particularly as the stimulus in bioimpedance measurement [1, 2]. The main advantage of chirps is the independent scalability in time and frequency domains: the duration of a pulse (usually short) and its frequency range (usually wide) can be adjusted separately. This feature is important in biomedical investigations for quick monitoring of the changing state of living tissue and cells.

The classical description of chirps presumes a sine-wave signal, instantaneous frequency $f(t)$ of which changes linearly in time. Consequently, the current phase $\theta(t) = \int f(t) dt$ of this chirp is changing in proportion to the square of time. The waveform of chirp expresses as $V_{ch}(t) = \sin(\theta(t)) = \sin(2\pi \int f(t) dt)$.

Generation of perfect sinusoidal chirps is an intricate task. Therefore, for simplifying generation and signal processing, applying chirps of the rectangular waveform with a small number of discrete amplitude levels should be preferred, e.g., for miniaturized measurement devices. Below we deal with such kinds of discrete-level chirp-like signals, known also as pseudo-chirps [2].

Bioimpedance measurement with chirp stimulus

The impedance of arbitrary biological matter or bioimpedance (BI), shortly, can be characterized by its electrical equivalent (EBI). The EBI is described mathematically by the frequency-dependent complex vector $\check{Z}(j\omega) = \text{Re}(\check{Z}(j\omega)) + j\text{Im}(\check{Z}(j\omega)) = |\check{Z}(\omega)| \exp(j\Phi_Z(\omega))$, where $\omega = 2\pi f$, $|\check{Z}(\omega)| = (\text{Re}(\check{Z}(j\omega))^2 + \text{Im}(\check{Z}(j\omega))^2)^{1/2}$, and $\Phi(\omega) = \arctg(\text{Im}(\check{Z}(j\omega))/\text{Re}(\check{Z}(j\omega)))$. Adjusting the parameters of excitation current I_{exc} through the bio-object, and measuring the response voltage V_z , we can find out the impedance spectrum of it as $\check{Z}(j\omega) = \mathcal{F}(V_z(t))/\mathcal{F}(I_{exc}(t))$, where \mathcal{F} denotes the Fourier Transform.

A possible architecture of the system for the EBI measurement is presented in Fig. 1 [3]. It executes the cross-correlation procedure (Corr) between the response

and reference signals, and thereupon calculates Fourier transform (FFT) of the cross-correlation function, i.e., the measurement of the unknown bioimpedance \check{Z} (or any complex impedance) is accomplished in succession $\text{Corr}(V_z, V_{ref}) \Rightarrow \text{FFT} \Rightarrow \{|\check{Z}(j\omega)|; \text{Im}(\check{Z}(j\omega))\}$. The result is a broadband impedance spectrum, which characterizes the difference between the EBI under study and the predetermined reference impedance \check{Z}_{ref} .

As a rule, the informative frequency bandwidth of the BI lies within the range from some kHz up to several MHz [1, 4]. The benefit of chirps is the simplicity of adjusting the sufficiently wide excitation range B_{exc} , which covers the frequency bandwidth of the object under measurement.

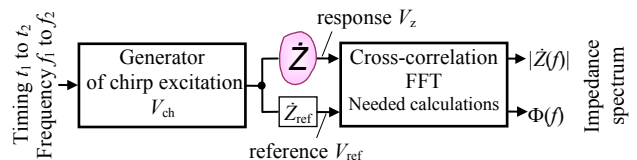


Fig. 1. Core structure of the 2-channel BI measurement system

In general, the manner of frequency change of chirps can be various: by a power function, exponentially, piecewise linearly, etc. We will pay the main attention to the first mentioned ones or so-called power chirps, the instantaneous frequency of which is changing according to the n -th order power function with arbitrary (*incl.* fractional) power n . This kind of sine-wave chirps with the amplitude A can be described mathematically as

$$V_{ch}(t) = A \sin\left(2\pi\left(f_0 t + \beta t^{n+1}/(n+1)\right)\right), \quad (1)$$

where $\beta = B_{exc}/T_{ch}$ characterizes the rate of frequency change (chirping rate), T_{ch} is the pulse duration, and $B_{exc} = f_{fin} - f_0$ with the final f_{fin} and initial f_0 frequencies.

Usually, chirps of many cycles (rotations of chirp-forming vector on the complex plane) are considered. However, it was shown in [5] that chirps of a single cycle or even less ($\theta(T_{ch}) \leq 2\pi$) can have the practical importance, if the very low power consumption or the extremely short

measurement time is required (implantable devices, lab-on-chips). The end frequencies, time duration and number of cycles of a chirp are strictly related. For the n -th order power chirps this relationship can be expressed as [5]

$$T_{\text{ch}} = L(n+1)/(nf_0 + f_{\text{fin}}), \quad (2)$$

where L is the number of cycles.

The basic discrete-level pseudo-chirp is the binary one (called also signum-chirp or Non-Return-to-Zero (NRZ) chirp), waveform of which represents the signum-function of the respective sine-wave chirp as $A \cdot \text{sgn}(V_{\text{ch}}(t))$, thus having values of $\{\pm A\}$ only – see Fig. 2a.

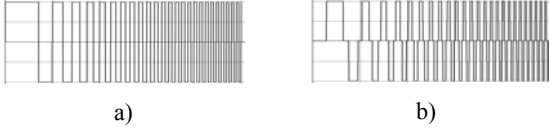


Fig. 2. Waveform of: (a) binary chirp; (b) ternary chirp

Another important class of pseudo-chirps is ternary (trinary) chirps or Return-to-Zero (RZ) chirps with the possible values of $\{+A; 0; -A\}$ – see Fig. 2b.

Unlike sine-wave chirps, the spectrum of the discrete-level ones is rippling intensively. Besides, the percentage of their in-band energy is somewhat less at the equal amplitude and duration of the pulse. In practice, these drawbacks should be compensated by the simplicity of the signal processing. An additional benefit of binary chirps is their unity crest factor, and consequently, major energy compared with the sine-wave chirps of the same length.

Next, let us examine some specific spectral features of both the mentioned modifications of linear pseudo-chirps ($n=1$).

Binary chirps with $f_0=0$

A specific feature of binary chirps is the gradually decreasing amplitude and power spectra by plateaus h ($h=1, 2, \dots$; Fig. 3). This effect and the energy distribution of binary chirps along the frequency spectrum, considering $f_0=0$, was discussed by the authors in [6] as follows.

The fundamental harmonic ($k=1$) of a rectangular signal with levels $\pm A$ has the root-mean-square (RMS) value $4A/(\pi\sqrt{2})$ and (presuming the unity load) the power $W_1 = (8/\pi^2)A^2$.

In the case of rectangular-wave chirps the fundamental harmonics from f_0 to f_{fin} are spread over the whole bandwidth B_{exc} , creating a constant value power spectral density (PSD) $w_1 = W_1/B_{\text{exc}}$, V^2/Hz . The power of every k^{th} higher odd ($k=3, 5, \dots$) harmonic $W_k = W_1/k^2$ is spread over the frequency range $B_k = kf_{\text{fin}} - kf_0 = kB_{\text{exc}}$ with PSD of $w_k = W_1/(B_{\text{exc}}k^2)$ – see Fig. 3a.

All the odd harmonic components contribute a certain part of their power for the first plateau ($h=1$) of the power spectrum with the width of B_{exc} (excitation power P_{exc}). It can be expressed as the sum

$$P_1 = P_{\text{exc}} = B_{\text{exc}} \sum_{k=1}^{\infty} w_k = W_1 \sum_{i=1}^{\infty} (2i-1)^{-3}. \quad (3)$$

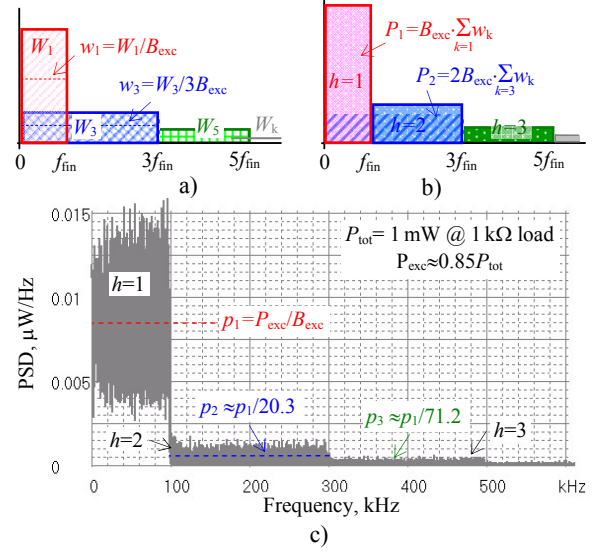


Fig. 3. (a) Power distribution of harmonic components; (b) power of spectral plateaus h ; (c) simulated power spectrum at $f_{\text{fin}}=100$ kHz

The power of every next plateau ($h>1$) with the width of $2B_{\text{exc}}$ is formed by the harmonics from $(2h-1)^{\text{th}}$ and higher, which expresses as (Fig. 3b)

$$P_h = 2W_1 \sum_{i=h}^{\infty} (2i-1)^{-3}. \quad (4)$$

The total power of all spectral plateaus outside the generated bandwidth is

$$P_{\text{out}} = \sum_{h=2}^{\infty} P_h = 2W_1 \sum_{i=2}^{\infty} (i-1)(2i-1)^{-3}. \quad (5)$$

For the first spectral plateau, the PSD $p_1 = P_1/B_{\text{exc}}$, while for all the next plateaus $p_h = P_h/(2B_{\text{exc}})$. The values of $p_1/p_h = 2P_1/P_h$ can be calculated by (3)–(5) – some of the results are shown in Table 1 and in Fig. 3c.

Table 1. The ratio of the PSD plateaus p_1/p_h

p_1/p_2	p_1/p_3	p_1/p_4	p_1/p_5	p_1/p_6
20.3	71.2	155.2	273.4	424.9

The total energy of the generated chirp signal is $E_{\text{tot}} = (P_{\text{exc}} + P_{\text{out}})T_{\text{ch}}$. However, it is essential to know not only the full energy, but also the amount of the energy E_{exc} , within the generated bandwidth (useful energy). Energy-efficiency of the generated excitation signal can be expressed as the ratio of $\delta_E = E_{\text{exc}}/E_{\text{tot}} = P_{\text{exc}}/(P_{\text{exc}} + P_{\text{out}})$. Using (3)–(5) yields [6]

$$\delta_E = \left(\sum_{i=1}^{\infty} (2i-1)^{-3} \right) / \left(\sum_{i=1}^{\infty} (2i-1)^{-2} \right) = 7\zeta(3)/\pi^2, \quad (6)$$

where ζ denotes Riemann's zeta-function.

The theoretical percentage of the useful energy by (6) is $\delta_E \approx 0.853$. In practice, the energy-efficiency of a signal can be evaluated from the results of FFT-processing as

$$\delta_E = \frac{\sum_{i=N_0}^{N_{fin}} |V_{ch}(\varphi_i)|^2}{\sum_{i=0}^{N_{max}-1} |V_{ch}(\varphi_i)|^2} \quad (7)$$

where $|V_{ch}(\varphi_i)|$ is the value of the amplitude spectrum at i^{th} frequency bin φ_i , N_0 and N_{fin} are the numbers of frequency bins, corresponding to the f_0 and f_{fin} , respectively. N_{max} is the total number of frequency bins of the FFT processing.

Some specific values for the chirps with length of 1000 cycles are presented in Table 2.

Table 2. Energy and power of chirps ($A=1$ V, $R_{load}=1$ k Ω)

Type of chirp	P , mW	E_{tot} , μ J	δ_E , %
sine-wave	0.5	10	99.8
binary	1.0	20	85.1
ternary 18°	0.8	16	93.1
ternary 30°	0.66	13.2	92.1

Binary chirps with $f_0 > 0$

When the initial frequency of a chirp $f_0 \neq 0$, then the shape of spectra becomes more complicated. Though the spectrum retains the gradual character, the shrinking of plateaus is not always monotonic. It depends on the ratio between f_0 and f_{fin} . In a certain case, one or more frequency sub-bands B_z with zero magnitude appear into a spectrum.

The forming of such a spectrum as the sum of its harmonics is explained by the draft diagram in Fig. 4a.

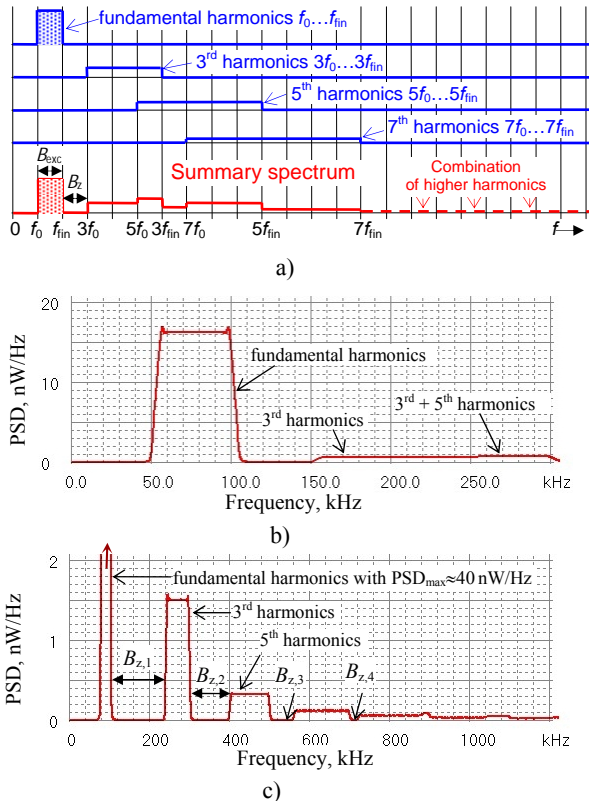


Fig. 4. (a) forming of spectrum at $f_0 \neq 0$; (b) power spectral density (PSD) of a binary chirp with $f_0=50$ kHz and $f_{fin}=100$ kHz; (c) fragment of the simulated PSD for $f_0=80$ kHz and $f_{fin}=100$ kHz

It is evident that fulfillment of the condition $3f_0 > f_{fin}$ produces the frequency area $B_{z,1} = 3f_0 - f_{fin}$ next to the

excitation bandwidth, where the spectrum has almost zero magnitude. In this specific case, the spectral density within the excitation bandwidth is determined only by the fundamental harmonic components from f_0 to f_{fin} . In general, the frequency area above f_{fin} can include more than a single zero sub-band, which separate spectral blocks of particular harmonics. Fulfilling of the condition

$$(2i+1)f_0 > (2i-1)f_{fin}, \quad i = 1, 2, 3, \dots \quad (8)$$

causes the zero-valued area from the frequency $(2i-1)f_{fin}$ up to $(2i+1)f_0$, i.e., $B_{z,i} = (f_{fin} + f_0) - 2i(f_{fin} - f_0)$ (Figs. 4b, 4c).

The condition (8) with $i=1$ has the more practical importance, assuring moderately wide, but distinctly separated excitation bandwidth – see simulated and smoothed spectrum in Fig. 4b, where $f_0=50$ kHz and $f_{fin}=100$ kHz. This condition with $i \geq 1$ simplifies evaluation of the energy-efficiency because the energy within the excitation bandwidth is always equal to the energy of first harmonic components from f_0 to f_{fin} only (see the discussion in the previous chapter)

$$\delta_E = T_{ch} W_1 / T_{ch} \sum_{k=1} W_1 / k^2 = 1 / \sum_{i=1} (2i-1)^{-2} = 8 / \pi^2. \quad (9)$$

Thus, in the case of binary chirps with $3f_0 > f_{fin}$ the theoretical energy-efficiency is constantly $\delta_E \approx 0.81$, i.e., it is equal to that of the common rectangular signal. Let us note that at $i \rightarrow \infty$ is equivalent to the $f_0 = f_{fin}$.

Ternary chirps

A method to improve the spectral properties of rectangular signals (*incl.* rectangular chirps) is shortening their duty cycle by a certain amount, thus modifying the binary signal to a ternary one (see Figs. 1b and 4) [7]. The shortening can be characterized by the relative time t/T_{ch} or by the equivalent phase angle α (for binary signals $\alpha = 0$) per a quarter of a period (or cycle), within of which the value of signal remains on the zero state (Fig. 5).

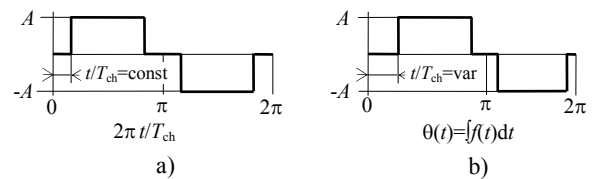


Fig. 5. Sketched ternary signals: (a) period of a signal with constant frequency; (b) cycle of a chirp

Let us explain the effect of shortening by Fourier series, which expresses for the rectangular-wave signal with the magnitude $\pm A$ as the sum of odd harmonics

$$F(\omega t) = \frac{4A}{\pi} \left[\sum_{i=1}^{\infty} \frac{\cos(2i-1)\alpha}{2i-1} \sin(2i-1)\omega t \right]. \quad (10)$$

As it follows from (10), the k^{th} harmonic ($k=2i-1$ with $i=1, 2, 3, \dots$) is absent from the series $F(\omega t)$, when $k\alpha = \pm(2i+1)\pi/2$, and $i=0, 1, 2, \dots$, because of $\cos(k\alpha)=0$. For example, $\alpha = \pi/6$, causes removing of the $(3+6i)^{\text{th}}$ harmonics, $\alpha = \pi/10$ removes the $(5+10i)^{\text{th}}$ harmonics, etc. This is valid for the rectangular chirps, too, but in this case

the time duration of every quarter-cycle is changing in accordance with the instantaneous frequency (Fig. 5b). Hence, in the generation of ternary chirps $V_{ch}(t)=\text{sgn}(\sin(\theta(t)))$ one must follow the current phase: if $2k\pi-\alpha<\theta(t)<2k\pi+\alpha$ or $(2k+1)\pi-\alpha<\theta(t)<(2k+1)\pi+\alpha$, ($k=0, 1, 2, \dots$), then $V_{ch}(t)=0$ (Fig. 6). Assuming numerical processing with sampling frequency f_{samp} , the current phase θ_i ($i=0, 1, 2, \dots, T_{ch}f_{\text{samp}}-1$) in degrees according to (1) expresses as

$$\theta_i = 360i(f_0 + \beta i / (2f_{\text{samp}})) / f_{\text{samp}} \cdot \quad (11)$$

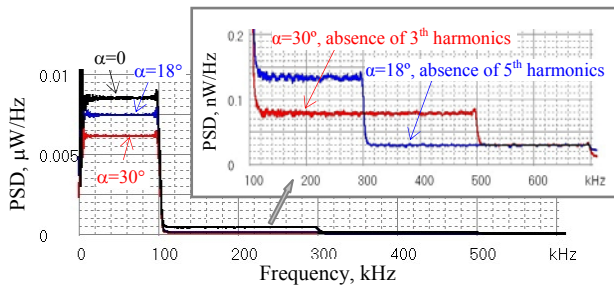


Fig. 6. Power spectral density (PSD) of ternary chirps at $\alpha=\text{var}$ with zoomed fragment of the outband spectra (smoothed curves)

Fractional-power (sub-linear) chirps

The previous examples indicated almost constant (on the average) spectral density within the excitation bandwidth (Figs. 3, 4, 6), but in biomedical studies it is sometimes practical to apply the stimulus with the spectral density rising with frequency. This effect can be achieved by using of sub-linear power chirps with the exponent n , slightly less than unity, for example, $n=0.8$ to 0.9 .

Conclusions

The chirp-wave excitation signal is highly convenient in bioimpedance measurements and impedance spectroscopy due to the possibility of fast and broadband identification of objects. Though the best measurement quality can be achieved by implementing the sine-wave chirp stimulus, the advantage of rectangular-wave signals is the simplicity of generation and processing of signals.

Aside the simpler hardware and software, another essential factor is energy consumption, which is extremely important in the development of miniaturized devices. That

is why the energy-efficiency of rectangular-wave chirps were analyzed in this work. It was shown, that the useful energy of discrete-level chirps is sufficiently high, exceeding 90% of the generated energy for ternary ones.

Depending on the aim and practicable needs, the shape of spectra can be simply modified by changing the initial frequency and duty cycle of generated chirps or selecting an appropriate mathematical basis of the signal.

The drawback of rectangular-wave chirps is their intensely rippling spectra, which can disturb the interpreting of measurement results. A way to overcome this issue is to focus on the phase spectra, in which the effect of rippling is diminished largely. This opportunity is more closely treated in the earlier works of authors [3].

Acknowledgements

This work was supported by the EU through the European Regional Development Fund, Estonian target-financed project SF0140061s12 and by Enterprise Estonia through the ELIKO Competence Center.

References

1. **Barsoukov E., MacDonald J. R.** Impedance Spectroscopy: Theory, Experiment, and Applications – New York: Wiley, 2005 – 595 p.
2. **Pollakowski M., Ermert H.** Chirp signal matching and signal power optimization in pulse echo mode ultrasonic nondestructive testing // IEEE Trans. Ultrason., Ferroelect. Freq. Contr., 1994 – No. 41(5). – P. 655–659.
3. **Min M., Paavle T., Ojarand J.** Time–frequency analysis of biological matter using short–time chirp excitation // Proc. European Conf. on Circuit Theory and Design (ECCTD2011), 2011. – P. 585–588.
4. **Grimnes S., Martinsen Ø. G.** Bioimpedance and Bio–electricity Basics – Elsevier–Academic Press, 2008. – 471 p.
5. **Paavle T., Min M., Ojarand J., Parve T.** Short–time chirp excitations for using in wideband characterization of objects: an overview // Proc. 12th Biennial Baltic Electronics Conf. (BEC2010), 2010. – P. 253–256.
6. **Min M., Paavle T., Annus P., Land R.** Rectangular wave excitation in wideband bioimpedance spectroscopy // Proc. IEEE 4th Int. Workshop on Medical Measurements and Applications (MeMeA2009), 2009. – P. 268–271.
7. **Min M., Kink A., Land R., Parve T., Rätsep I.** Modification of pulse wave signals in electrical bioimpedance analyzers for implantable medical devices // Proc. 26th Annual Intern. Conf. EMBS’2004. – IEEE, 2004. – P. 2263–2266.

Received 2012 03 19

Accepted after revision 2012 04 17

T. Paavle, M. Min. Discrete-Level Broadband Excitation Signals: Binary/Ternary Chirps // Electronics and Electrical Engineering. – Kaunas: Technologija, 2012. – No. 6(122). – P. 23–26.

This research deals with using of discrete-level chirp signals as the excitation ones for bioimpedance measurement. Discrete-level (binary, ternary) chirps simplify the necessary hardware and software in the development of respective devices essentially, but assure the wide frequency range measurements and high energy-efficiency at the same time. Mostly the chirps with instantaneous frequency, which is changing by a power function, is treated. Ill. 6, bibl. 7, tabl. 2 (in English; abstracts in English and Lithuanian).

T. Paavle, M. Min. Diskretaus lygio plačiajuosčiai dvigubi arba trigubi čirškimo sužadinimo signalai // Elektronika ir elektrotechnika. – Kaunas: Technologija, 2012. – Nr. 6(122). – P. 23–26.

Nagrinėjama, kaip diskretaus lygio čirškimo signalus panaudoti bioimpedansui matuoti. Naudojant diskretaus lygio (dvigubus, trigubus) čirškimo signalus pakanka paprastesnės būtinios aparatinės ir programinės įrangos, kuriant atitinkamus įtaisus, o kartu užtikrinami plačios dažnių juostos matavimai ir didelis energetinis efektyvumas. Il. 6, bibl. 7, lent. 2 (anglų kalba; santraukos anglų ir lietuvių k.).